

Rapid Changes of Magnetic Fields Associated with Six X-class Flares

Haimin Wang, Thomas J. Spirock, Jiong Qiu, Haisheng Ji, Vasyl Yurchyshyn, Yong-Jae Moon, Carsten Denker and Philip R. Goode

*Big Bear Solar Observatory, New Jersey Institute of Technology
40386 North Shore Lane, Big Bear City, CA 92314-9672*

haimin@flare.njit.edu -- Version on April 8, 2002

ABSTRACT

In this paper, we present the results of the study of six X-class flares. We found significant changes in the photospheric magnetic fields associated with all of the events. For the five events in 2001, when coronagraph data were available, all were associated with Halo CMEs. Based on the analyses of the line-of-sight magnetograms, all six events had an increase in the magnetic flux of the leading polarity of order of a few times 10^{20} Mx while each event had some degree of decrease in the magnetic flux of the following polarity. The flux changes are considered impulsive, as the “change-over” time, which we defined as the time to change from pre-flare to post-flare state, ranged from 10 to 100 minutes. The observed changes are permanent. Therefore, the changes are not due to changes in the line profile caused by flare emissions. For the three most recent events, when vector magnetograms were available, two showed an impulsive increase of the transverse field strength and magnetic shear after the flares, as well as new sunspot area in the form of penumbral structure. One of the events in this study was from the previous solar cycle. This event showed a similar increase in all components of the magnetic field, magnetic shear and sunspot area. We present three possible explanations to explain the observed changes: (1) the emergence of very inclined flux loops, (2) a change in the magnetic field direction and (3) the expansion of the sunspot which moved some flux out of Zeeman saturation. However, we have no explanation for the polarity preference, i.e. the flux of leading polarity tends to increase while the flux of following polarity tends to decrease slightly.

Subject headings: Sun: activity – Sun: flares – Sun: magnetic fields

1. INTRODUCTION

The evolution of photospheric magnetic fields before, during and after solar flares is extremely important, but not well understood. Even though many authors have studied the problem for nearly four decades, the results, thus far, have not been conclusive. While some authors reported a decrease in the strength of the magnetic field after, and presumably associated with, solar flares (Severny 1964; Zvereva & Severny 1970; Moore et al. 1984; Kosovichev & Zharkova 1999, 2001), some others argued that the changes are consistent with a general trend in the evolution of the magnetic fields of active regions. (see Sakurai & Hiei, 1996 for a review).

It has been established, from the early studies of the relationship of solar flares to the morphology of an active region's magnetic field, that strong flares mostly occur near the neutral lines of the active region's vertical component of the magnetic field where there is a strong gradient in magnetic field and where the horizontal component is strongly sheared. This shear in the horizontal component may experience substantial flare-related changes. Wang et al. (1994) determined that the magnetic shear of an active region may increase after the occurrence of an X-class flare. This result initially appears to be counter-intuitive as the magnetic shear is expected to decrease as the total magnetic energy of the active region decreases. Chen et al. (1994) studied more than 20 M-class flares and determined that there was essentially no apparent change in magnetic fields associated with the flares. The results from studies conducted at the Marshall Space Flight Center (Ambastha et al., 1993; Hagyard et al, 1999) showed inconclusive results. The morphology of an active region's magnetic field may or may not change as the result of a solar flare and the magnetic shear in the active region may decrease, increase or remain unchanged.

Two very recent papers provide some key understanding of this subject. Kosovichev and Zharkova (2001) studied high resolution MDI magnetogram data for the 2000 July 14 "Bastille Day Flare" and found both a permanent decrease in magnetic flux and a short-term magnetic transient. The first phenomenon was explained by the release of magnetic energy and the second by high-energy electrons bombarding the solar surface. Spirock et al. (2002) studied the X20 flare on April 2, 2001, the largest solar flare in the last few decades, and found that, after the flare, the magnetic flux of the leading polarity increased by approximately 6×10^{20} Mx, while there was no obvious change in the magnetic flux in the following polarity. Two explanations were offered. The observed changes were the result of new flux emergence, and/or a change of the direction of the field from more vertical to more tangential.

Motivated by the recent advances in this topic, the remaining inconsistencies in the results and the recent upgrade of the Vector Magnetograph system at the Big Bear Solar

Observatory (BBSO), in addition to the aforementioned X20 flare, we studied 4 recent X-class flares and re-examined the X9 flare of March 22, 1991, which was previously studied by Wang and Tang (1993). In this paper, we summarize these six events and find that unbalanced, rapid and permanent flux increase might be a common property of major solar flares. As these flares were associated with fast Halo CMEs, our observations may also provide clues to the understanding of the mechanisms which trigger CMEs.

2. OBSERVATIONS AND DATA REDUCTION

The data that we are presenting include magnetograms, optical filtergrams and X-ray emission flux curves to show the location, magnetic morphology and temporal evolution of the flares under study. We now discuss the five different data sets used in this study.

(1) For four out of the six events, we used data from BBSO’s Digital Vector Magnetograph (DVMG) system, which typically covers an area of about $300'' \times 300''$. This new system has a much improved sensitivity and resolution compared to that of the old BBSO Videomagnetograph system. The hardware has been described in detail by Spirock et al. (2002). It consists of a $1/4 \text{ \AA}$ band pass filter, an SMD 1024×1024 12-bit CCD camera and three liquid crystals used as polarization analyzers. Each data set consists of four images: 6103 \AA filtergram (Stokes-I), line-of-sight magnetogram (Stokes-V) and the transverse magnetogram (Stokes-U and -Q). We usually rebin the camera to the 512×512 mode to increase the sensitivity of the magnetograms. After rebinning, the pixel resolution is about $0.6''$. The line-of-sight magnetic sensitivity is approximately 2 Gauss while the transverse sensitivity is approximately 20 Gauss. The cadence for a complete set of Stokes images is typically 1 minute.

In this paper, we compare the study of the line-of-sight magnetograms for all of the events. For the three events for which vector magnetograms are available, we will only present the results of which we are confident. For each vector magnetogram, we correct the cross-talk by scatter plots of Stokes V vs. Q and V vs. U. Because the current DVMG system at BBSO does not use any mirrors, the instrumental polarization is negligible. The 180-degree ambiguity in the direction of the vector is resolved by comparing the vector magnetograms with the extrapolated potential fields using the line-of-sight field as the boundary condition. Although the resulting vector maps look reasonable, the potential field method is not sufficient for more quantitative studies such as the analyses of electric currents and the 3-D structure of magnetic fields. A more detailed study of these data sets will be published in a sequence of follow-up papers.

(2) For one of the events (April 6, 2001), we did not have BBSO data. Therefore, we used high resolution, high cadence line-of-sight magnetograms from the Michelson Doppler Imager (MDI) on board the Solar and Heliospheric Observatory (SOHO). MDI mainly obtains full-disk dopplergrams for the investigation of solar oscillations. In addition, MDI provides full disk longitudinal magnetograms with a cadence of 1 minute and an image scale of 2" (Scherrer et al., 1995).

(3) To show the spatial structure and temporal evolution of the flares, we also used both high resolution and full-disk $H\alpha$ images from BBSO, hard X-ray time profiles from the Yohkoh Hard X-ray Telescope (HXT) as well as from its Wide Band Spectrometer (WBS).

(4) For the August 25, 2001 event, we used high resolution and high cadence white light data from the Transition Region and Coronal Explorer (TRACE) to study the sunspot evolution. We use them to compare with the white light data from BBSO observations, to ensure that the two data sets agree. TRACE 171Å images were used to determine the location of the flare ribbon of the April 6, 2001 event.

(5) C2 and C3 coronagraph data from the Large Angle Spectrometric Coronagraph (LASCO) on board SOHO were used to check the nature of the CMEs, if there is one, associated with the particular flare under study. LASCO data were only available for the five events in 2001. No coronagraph data was available for the March 22, 1991 event.

3. RESULTS

For each event, we started with the analyses of the line-of-sight magnetograms. To determine the location of any obvious changes in the active region's magnetic field, we created movies of the line-of-sight magnetic field from well before to well after each particular event. We then choose two regions of study for each event. The first region encompasses the flare. Then, to ensure that any changes seen were not the result of external or instrumental effects, such as varying seeing, problems with the liquid crystals or filter, etc., we chose a control region that was away from the location of the flare and did not display any temporal changes in the magnetic field as a result of the flare. We then plotted both the positive and negative flux in the flaring region, normalized by the reference region. As we shall see, the rapid changes are localized for some cases but are spread over the entire sunspot region for other cases.

Table 1 provides an overview of these six events. It includes the time of the flares, NOAA active region number, the GOES X-ray classification, the location on the disk, time-scale and the amount the magnetic flux changed. Please note the 1st (March 22, 1991) and 2nd

(April 2, 2001) events have been discussed in detail in two previous papers (Wang and Tang, 1993 and Spirock et al., 2001, respectively). From the table, we note a common property shared by all of the events: there is an impulsive and permanent increase of the magnetic flux in the leading polarity only. In all cases, the flux of following polarity tends to decrease to some extent.

In Table 1, “S Time” is the flare starting time as determined from Solar Geophysical Data (SGD), “P time” is the time of the flare peak, “Loc.” is the heliospheric coordinates, in degrees, of the active region; “ ΔT ” is the time it took for the flux to change from the pre-flare level to the post-flare level (change-over time), “ ΔP ” is the amount of flux change for the preceding (leading) polarity and “ ΔF ” is the flux change for the following (trailing) polarity.

Next, let us discuss six events in detail. We first will discuss four events that may be due to emergence of inclined flux ropes, and then two events that may be due to expansion of p spots after the flare.

3.1. August 25, 2001 X5.3 Flare

This flare exhibited the most impulsive changes among the six flares considered in this paper. The flux “change over” was completed within 10 minutes. For this event, we can pinpoint the area of new flux appearance. It is the area along the neutral line as marked by the white box in Figure 1. As shown in Figure 2, the leading (negative) flux in this box increased by about 1.8×10^{20} Mx, while the following (positive) flux decreased by 0.8×10^{20} Mx. The transverse field strength in this region also experienced a rapid increase on the order of 70 Gauss. The weighted mean magnetic shear angle rapidly increased by 10 degrees. This shear angle is defined as the angular difference between the potential and the measured transverse fields, weighted by the measured transverse field strength. Note that, as shown in the bottom panel of Figure 2, the mean intensity of the box decreased gradually, beginning immediately after the flare, indicating the formation of new sunspot area. The mean intensity of 1.0 indicates the mean photospheric intensity outside of the sunspots. Both BBSO and TRACE white light movies show the formation of new sunspot area clearly. Figure 3 shows four TRACE white light images. The arrow denotes the formation of new sunspot area, which is predominantly in the form of penumbra.

3.2. October 19, 2001 X1.6 Flare

Figure 4 shows the magnetic configuration and flare morphology of the October 19, 2001 event. Again, in Figure 5, we plot the magnetic field changes in the area marked by the box in Figure 4. The trend of the changes for this flare is very similar to that of the August 25, 2001 flare. However, the “change over” is rather gradual. The amount of flux increase in the leading polarity (positive) was 3.0×10^{20} Mx while the following (negative) flux decreased by 0.4×10^{20} Mx, over the time scale of 60 min. We found that the decrease of the following flux is primarily due to the cancellation of the newly formed positive flux with the previously existing negative flux around the leading spot.

For this event, the increase in the transverse field has the same trend as that of the line-of-sight field. The mean value of the transverse field in the calculation box increased by 90 Gauss. The weighted mean shear angle increased by almost 10 degrees. The increase of the shear angle occurred during a period of 15 minutes, which was much more rapid than that of the change in the line-of-sight and transverse field strength. In the bottom panel of Figure 5, we plot the mean intensity of the box. The mean photospheric value is defined as 1.0. Therefore, the decreasing intensity indicates the appearance of new sunspot area. As is the case with the August 25, 2001 event, the evolution of the magnetic shear is also impulsive and permanent. Also, similar to the August 25, 2001 event, the new sunspot area is in the form of penumbra.

In Figure 6, we compare the vector magnetograms before and after this flare. The thick black lines are the magnetic neutral lines. The neutral line which runs approximately horizontally across the images at about $y = 45''$ is the primary location of the increase in magnetic field strength and shear angle.

This is another clear example of new flux appearance immediately following a flare. As we will discuss later, our explanation for the observed changes in each active region’s magnetic flux requires that the new flux be very inclined to allow the appearance of only one polarity.

3.3. April 2, 2001 X20 Flare

This flare was studied extensively by Spirock et al. (2002), using both BBSO and MDI data. This was the only one of the six events that was very close to the limb (65 degrees West). The leading (limbward, positive) flux increased by 6×10^{20} Mx, while the following (diskward) flux basically remained unchanged or, perhaps, decreased slightly (1.5×10^{20} Mx, which is about the noise level of the measurement). The authors suggested two possible

theories to explain this event: (1) the emergence of a very inclined flux loop and (2) a change in the direction of the magnetic field from more vertical to a more inclined orientation.

There are some limitations to these explanations. Please refer to the discussions in Section 4. Because the region was close to the limb, and there were no transverse magnetic field observations, the slight decrease of following flux was difficult to explain. Using the experience gained from our study of other events discussed in this paper, all of which took place near disk center, we postulate that the decrease of the magnetic flux of the following polarity could be due to flux cancellation by some of the newly emerged leading flux with the opposite polarity that previously existed.

3.4. Re-evaluation of the March 22, 1991 X9 Flare

Wang and Tang (1993) discussed this flare in detail and found that there was an increase in the leading (positive) flux by 10^{20} Mx. They were unable to detect any change in the following (negative) flux. The negative flux was mostly encompassed within the the major sunspot. The BBSO Videomagnetograph (VMG) system is not able to measure large sunspot umbral fields accurately due to Zeeman saturation and the reduced light level of the sunspot’s umbra. Due to these limitations, any change in the strength of the negative component of the magnetic field remains undetermined.

As noted when we compare the results of this event with the results of the other events, the lack of change of the flux in the following polarity may be true and not due to observational and instrumental effects. For this event, the authors claimed that abrupt flux emergence was the likely cause of the flux increase. The appearance of new sunspot area, coinciding with the flux increase, supports this argument. In addition, the magnetic shear along the active region’s neutral line increased impulsively.

3.5. April 6, 2001 X5.6 Flare

For this event there were no BBSO magnetograms available. Therefore, we used MDI magnetograms to calculate the changes in the magnetic flux. Figure 7 shows a magnetogram one half hour before the flare (left panel), as well as the flare morphology as seen in the TRACE 171Å observation (right panel). The box in the magnetogram marks the region of the flux calculation.

Figure 8 shows the evolution of the positive and negative magnetic flux. The Yohkoh WBS hard X-ray plot is superimposed on the magnetic flux plots to indicate the timing of the

flare. The following (positive) flux decreased by 4×10^{20} Mx while the leading (negative) flux increased by 4×10^{20} Mx. This is the only event in this study where we found a substantial decrease in the flux of the following polarity. It appears that this flux change is over the entire sunspot area. The flux reduction of both polarities, during the flare, is likely due to line weakening, although Kosovichev & Zarkova (2001) explained that it is caused by the bombardment of the solar surface by high energy electrons. However, the study of the evolution of flux during the impulsive phase of a flare is not an essential topic for this paper.

3.6. October 22, 2001 X1.6 Flare

For this event, we were not able to pin down the exact location of the flux change after the flare. It appears that the entire leading spot grew in size and added a leading (negative) flux in the amount of 12×10^{20} Mx, while the following (positive) flux dropped by 2×10^{20} Mx. Figure 9 shows the magnetogram (left panel), white-light (center panel) and $H\alpha$ (right panel) images for this event. The flux calculation was based on the entire $120''$ by $120''$ window. Figure 10 shows the evolution of the flux, along with the Yohkoh HXT curve to indicate the time of the flare. There were no obvious impulsive changes of the transverse magnetic field, mean intensity or shear angle. Therefore, these parameters were not included.

4. SUMMARY AND DISCUSSION

There are two common properties to these six X-class flares:

- (1) There was an impulsive and permanent change in the magnetic flux associated with each flare.
- (2) The leading flux always increased while the following flux tended to decrease, though by a much smaller amount.

For four of the events we can pinpoint a small area where the flux changed, this area is always at the core of the flaring neutral line. For the two additional events the change appears to have been more uniform over the entire sunspot area.

We immediately face a difficult problem. If a region is close to the disk center, Maxwell's law requires that the flux emergence should be balanced. The positive and negative flux should increase by the same amounts, unless the new flux is extremely inclined. It does not seem possible for one polarity to increase and the other to decrease.

In the paper by Spirock et al. (2002), we explained the unbalanced flux increase for the

April 2, 2001 event by two possible mechanisms:

(1) With the emergence of a very inclined flux tube, only the limbward polarity would show a flux increase. This scenario can explain some signatures of flux emergence, such as the appearance of the new umbral area associated with the March 22, 1991, the August 25, 2001 and the October 19, 2001 flares. However, this suggestion could not explain the decrease of flux in the following polarity. We now realize that the decrease in the following flux could be due to flux cancellation between newly emerged leading flux and previously existing following flux. The August 25 and October 19, 2001 events both showed the best proof of this.

The new flux emergence could be the result of a relaxation of magnetic energy in the upper atmosphere, which would enable the subsurface flux to emerge more easily. The increase of magnetic shear signifies that the newly emerged flux is also sheared. We also note that the shear increase was predicted by Melrose (1995) as a result of the relocation of DC currents to the lower atmosphere from higher up in the corona after a flare.

(2) The unbalanced flux increase could also be the result of a change in the orientation of the magnetic field. For the limb event of April 2, 2001 the field would become more inclined in the leading polarity after the flare. However, for all other events discussed in this paper, the flares were close to disk center. Therefore, the increase in the leading polarity's line-of-sight flux requires the field in that location to become more vertical after the flare, while the decrease of the line-of-sight component of the following flux would require the field, in that location, to become more inclined. The vector magnetograph observations for the August 25, and October 19, 2001 do not support this explanation.

We can also offer a third explanation:

(3) After the relaxation of the magnetic field in an active region, the preceding sunspot may expand slightly. The other way to look at this is that the electric current of the sunspot decreased after a flare, causing pinch force to decrease. Therefore, the spot to expand. The actual flux will not increase due to this effect. However, some flux may move out of the umbral area that had more Zeeman saturation before the flare. Therefore, more flux will become detectable after the flare. The results of the April 6 and Oct. 22, 2001 events seem to support this view. Even though this may be due to an observational effect, the sudden expansion of p-spots after a major flare deserves theoretical explanation.

Table 2 summarizes the change of magnetic shear and possible explanation(s) for all six events.

In addition, there is no existing theory to explain why the leading flux area should

preferentially experience flux increase. We really do not have a unified theory to explain what we observed here, even though each event can be explained by one or two theories. We are confident that our observational results are substantially above any systematic errors.

For all of the five events in 2001, we had C2 and C3 coronagraph data from LASCO. All of these events were associated with Halo CMEs. Therefore, the understanding findings here would help us to understand the mechanism responsible for triggering CMEs. As an example, we would like to mention the erupting flux rope model (Chen, 1989; Chen and Garren, 1993; Krall et al., 2001). This model predicts an increase of tangential magnetic flux associated with a CME. However, the details of the model’s parameters (e.g., time scale and amount of flux emergence) need to be carefully compared with our observations.

We are grateful to the BBSO observing staff for their support in obtaining the data. The work is supported by NSF under grants ATM-0076602, ATM-9903515 and ATM-0086999, AST-9987366, NASA under grants NAG5-9682, NAG5-9738 and NAG5-10910, and ONR under grant N00014-97-1-1037.

Table 1. Overview of Flares

Date	S Time	P Time	AR No.	Size	Loc.	ΔT	ΔP (Mx)	ΔF (Mx)
03/22/91	2230UT	2247UT	6555	X9.0	S23E20	50min	$+1 \times 10^{20}$	0
04/02/01	2132UT	2151UT	9393	X20	N19W65	100min	$+6 \times 10^{20}$	-1.5×10^{20}
04/06/01	1910UT	1921UT	9415	X5.6	S20E31	40min	$+4 \times 10^{20}$	-4×10^{20}
08/25/01	1623UT	1645UT	9591	X5.3	S17E34	10min	$+1.8 \times 10^{20}$	-0.8×10^{20}
10/19/01	1613UT	1630UT	9661	X1.6	N15W29	60min	$+3 \times 10^{20}$	-0.4×10^{20}
10/22/01	1744UT	1759UT	9672	X1.2	S18E16	60min	$+11 \times 10^{20}$	-2×10^{20}

Table 2. Explanation of Findings

Date	Magnetic Shear	CME	New Spot	Explanation(s)
03/22/91	Increase	Unknown	Yes	(1)
04/02/01	No Vector Data	Partial Halo	No	(1 and 2)
04/06/01	No Vector Data	Halo	No	(3)
08/25/01	Increase	Halo	Yes	(1)
10/19/01	Increase	Halo	Yes	(1)
10/22/01	No change	Halo	No	(3)

REFERENCES

- Ambastha, A., Hagyard, M.J. and West, E.A., 1993, Sol. Phys., 148, 277
- Chen, J., 1989, Ap.J., 338, 453
- Chen, J. & Garren, F., 1993, GRL, 20,2319
- Chen, J., Wang, H., Zirin, H. & Ai, G. 1994, Sol. Phys., 154, 261
- Hagyard, M.J., Start, B.A., and Venkatakrishnan, P., 1999, Solar Physics, 184, 133
- Kosovichev, A. G., & Zharkova, V. V. 1999, Sol. Phys., 190, 459
- Kosovichev, A. G. & Zharkova, V.V., 2001, Ap. J. Letters, 550, L105
- Krall, J., Chen, J., Duffin, R.T., Howard, R.A. & Thompson, B.J., 2001, Ap. J., 562, 1045
- Melrose, D.B., 1995, Ap. J., 451, 391
- Moore, R. L., Hurford, G. J., Jones, H. P., & Kane, S. R. 1984, ApJ, 276, 379
- Sakurai, T., & Hiei, E. 1996, Adv. Space Res., 17, 91
- Scherrer, P. H., et al. 1995, Sol. Phys., 162, 129
- Severny, A. B. 1964, ARA&A, 2, 363
- Spirco, T. J., Yurchyshyn, V. & Wang, H., 2002, Ap. J., in press
- Wang, H. & Tang, F., 1993, ApJ Letters, 407, L89
- Wang, H., Ewell, M. W., Zirin, H. & Ai, G. 1994, ApJ, 424, 436
- Zvereva, A. M., & Severny, A. B. 1970, Izv. Krymskoi Astrofiz. Obs., 4142, 97

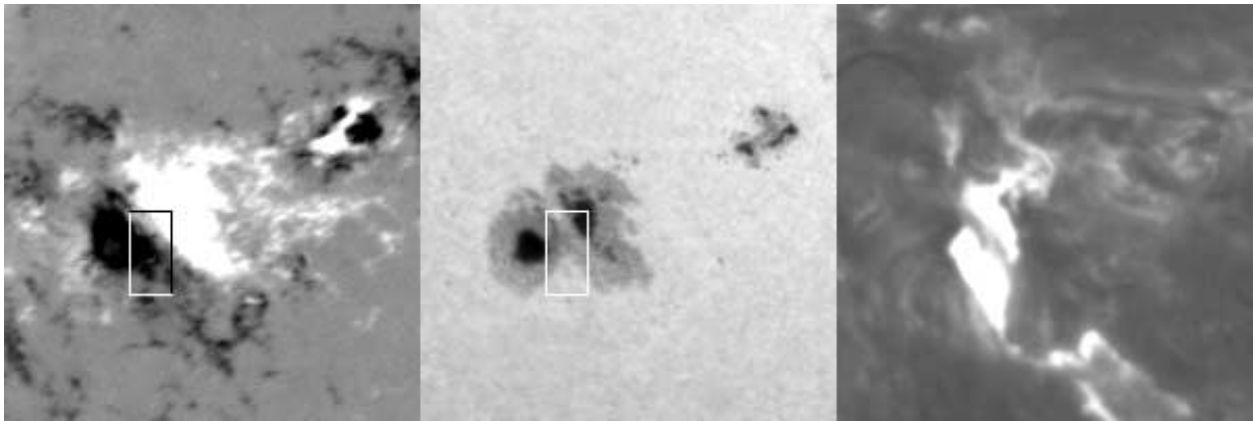


Fig. 1.— Line-of-sight magnetogram, white-light and H α images of the August 25, 2001 flare which occurred in AR 9591. The field view is $190'' \times 190''$. The box marks the flux calculation area. The H α image shows the morphology of the flare.

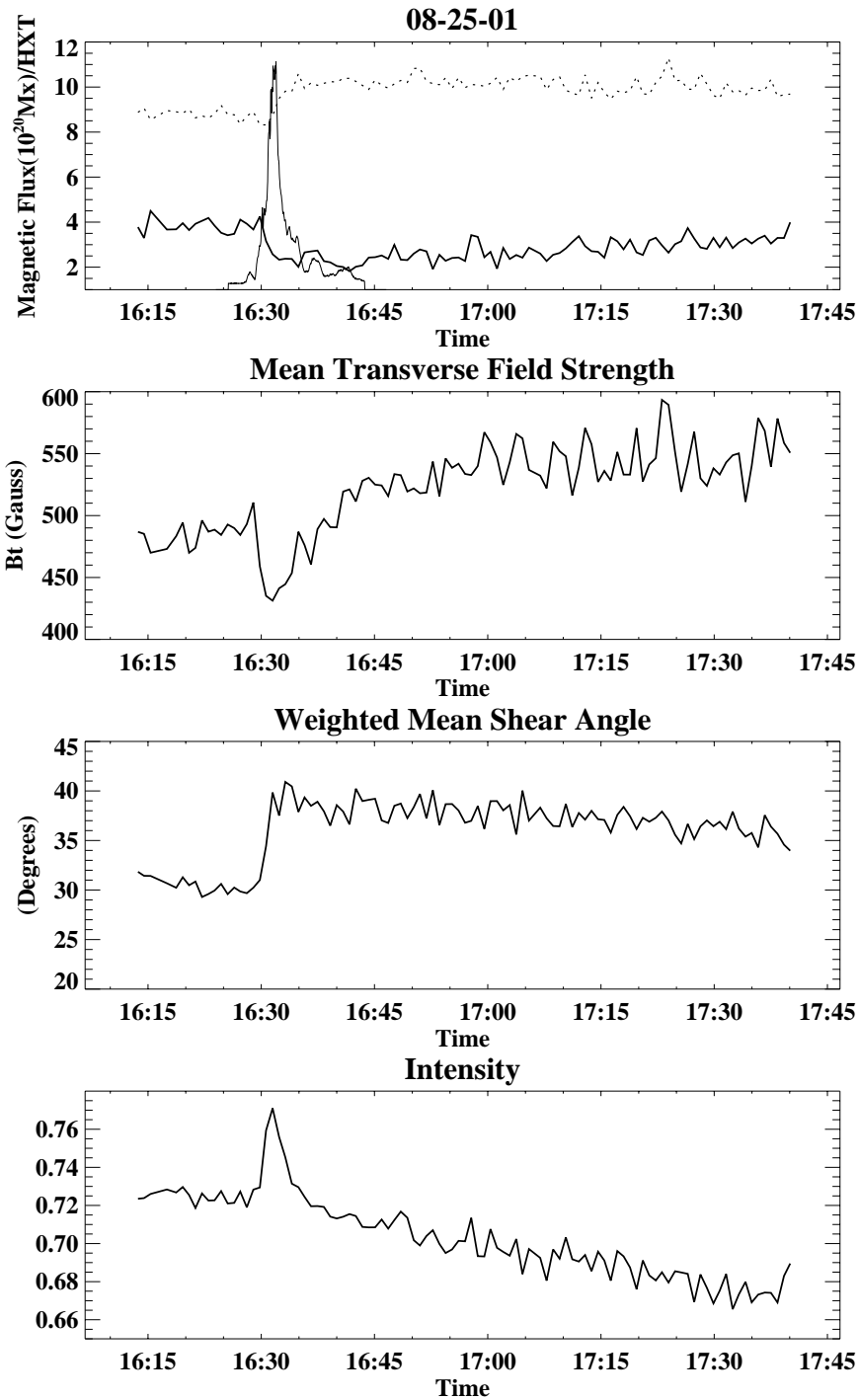


Fig. 2.— The first panel shows the evolution of magnetic flux in AR 9591 on August 25, 2001. The solid line represents the following (positive) flux while the dashed line represents the leading flux (negative). The solid thin line is the YOHKOH hard X-ray curve in high energy channel of HXT. Second panel: evolution of transverse field strength. Third panel: weighted mean shear angle. Bottom panel: mean intensity in the box.

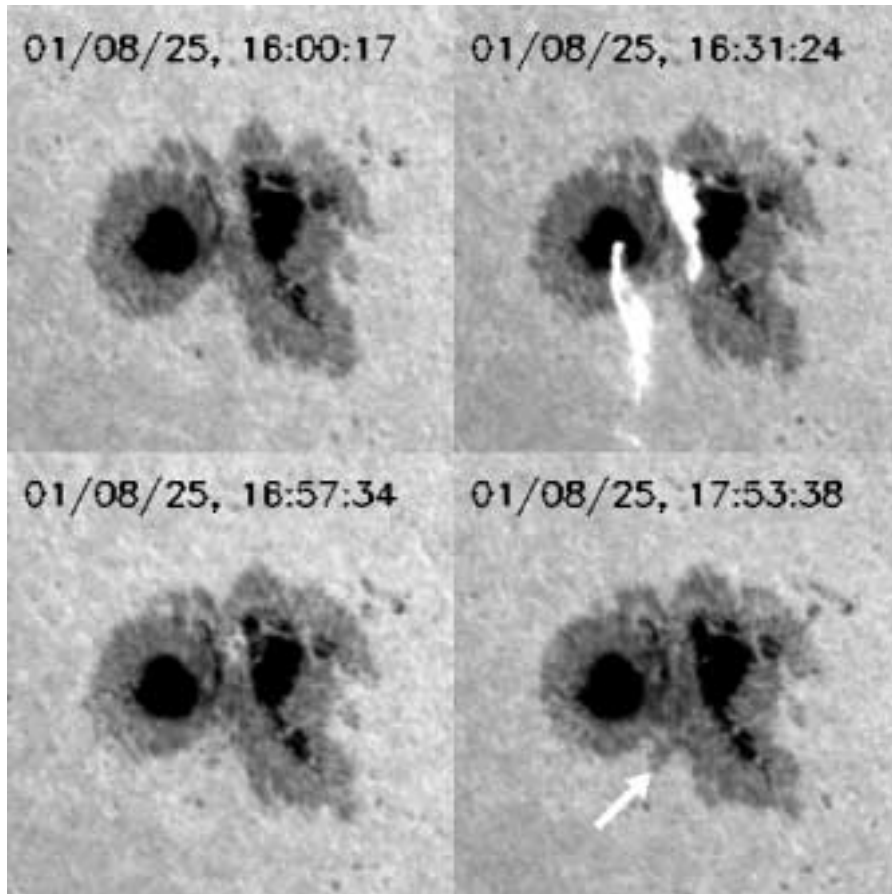


Fig. 3.— A sequence of TRACE images showing the August 25, 2001 flare. The new penumbral area is indicated by the arrow. The time of the flare maximum is approximately 16:32UT.

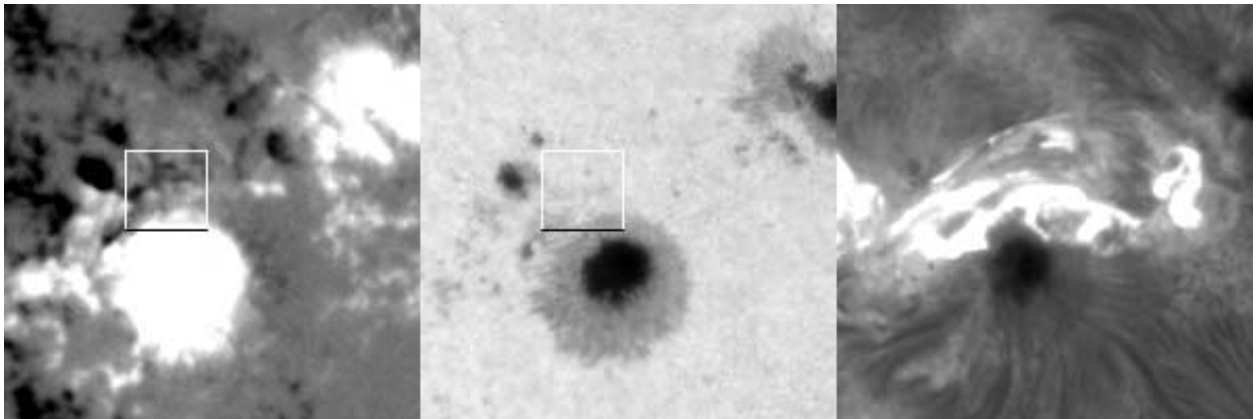


Fig. 4.— The line-of-sight magnetogram, white-light and $H\alpha$ images for the flare of October 19, 2001 which occurred in AR 9661. The field of view is $120'' \times 120''$. The box marks the flux calculation area. $H\alpha$ image shows the morphology of the flare.

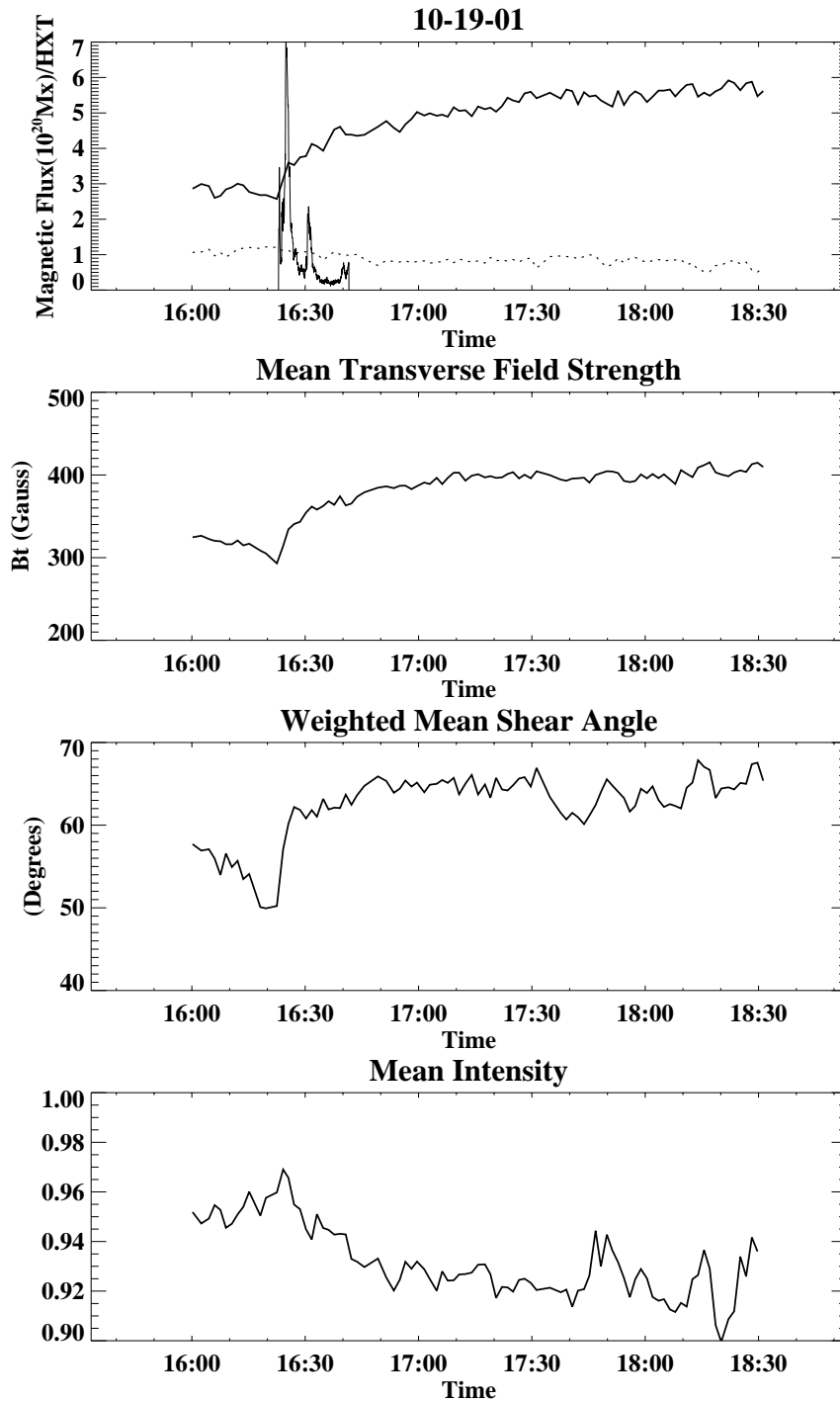


Fig. 5.— The first panel shows the evolution of magnetic flux on October 19, 2001. The solid line represents the leading (positive) flux while the dashed line represents the following flux (negative). The thin solid line is the YOHKOH hard X-ray curve in high energy channel of HXT. Second panel: evolution of transverse field strength. Third panel: weighted mean shear angle. Bottom panel: mean intensity in the box.

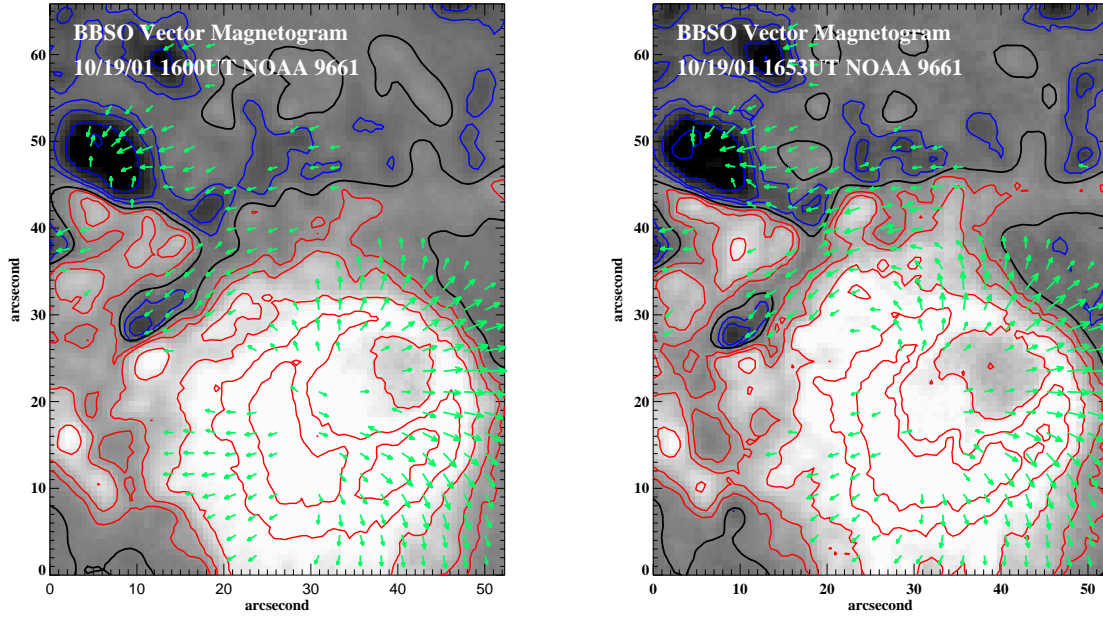


Fig. 6.— Vector magnetograms of October 19, 2001 of AR 9661. The left panel shows the magnetic fields before the flare, while the right panel shows the magnetic fields after the flare. Gray scale represents line-of-sight magnetic field strength which is also plotted as contours (red: positive field, blue: negative). The green arrows indicate transverse fields. The dark black lines are the magnetic neutral lines where the line-of-sight field is zero.

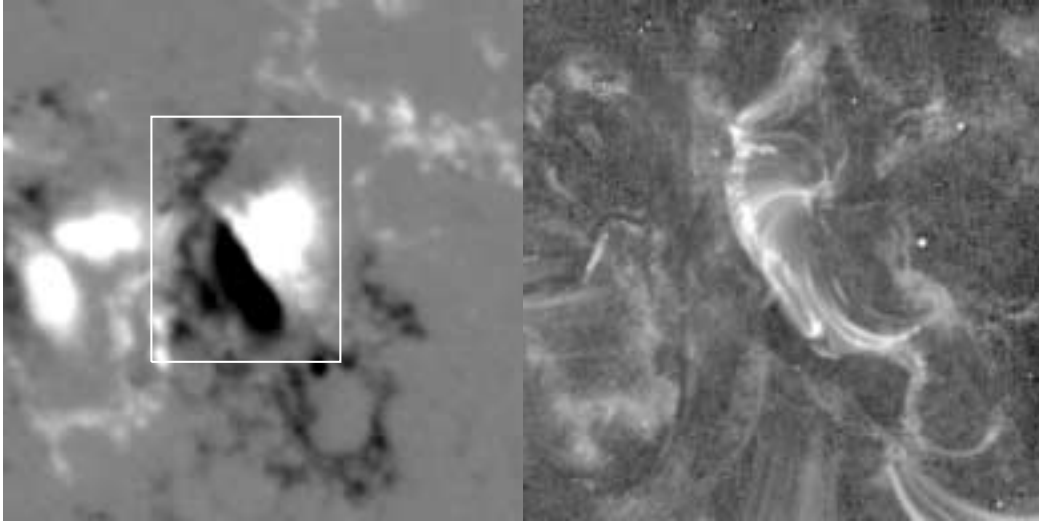


Fig. 7.— The left panel shows the line-of-sight magnetogram of April 6, 2001 of AR 9415. The box marks the flux calculation area. The right panel is the TRACE 171Å image during the flare. The field of view is 200×200 arcsec.

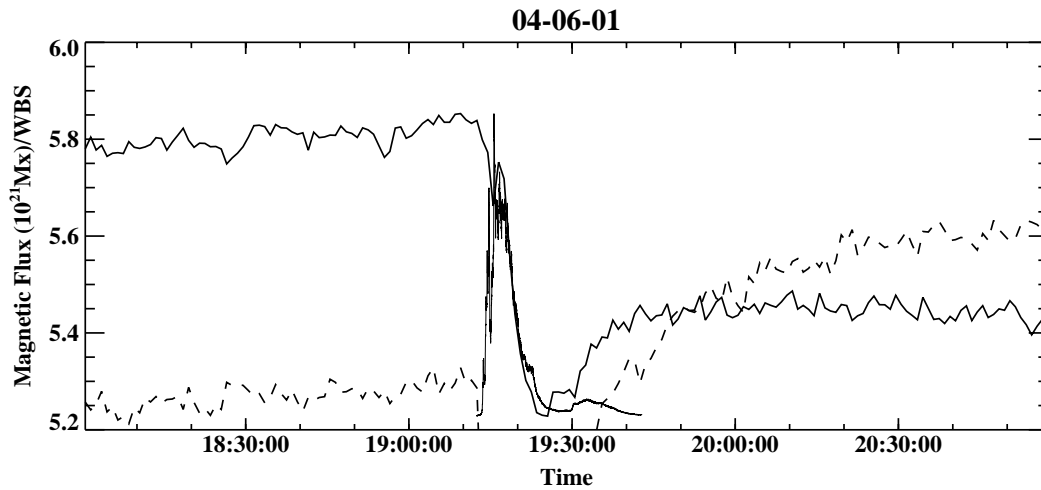


Fig. 8.— The evolution of negative (leading polarity, dashed line) and positive (following polarity, thick solid line) magnetic flux in AR 9415 on April 6, 2001. The thin solid line is the YOHKOH/WBS hard X-ray curve.

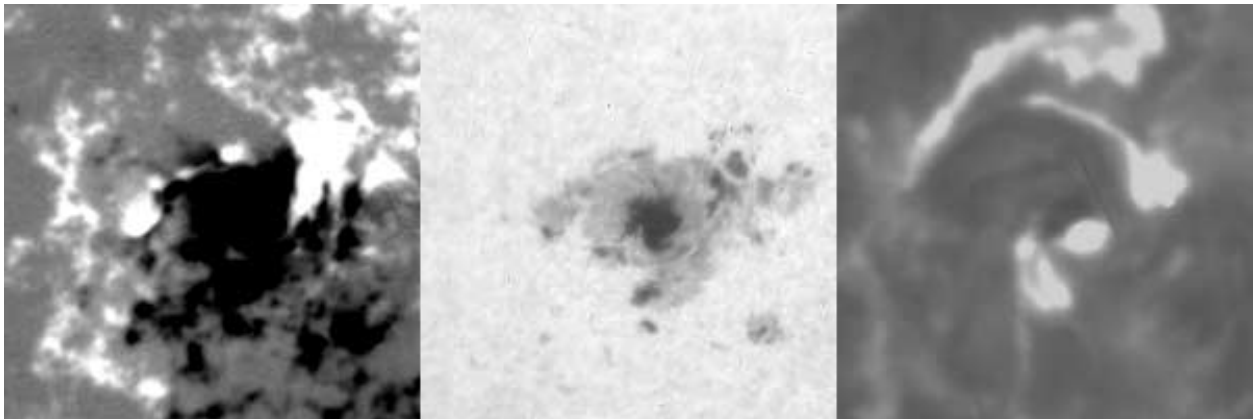


Fig. 9.— The line-of-sight magnetogram, while-light and $H\alpha$ images of the October 22, 2001 flare which occurred in AR 9672. The field of view is $120'' \times 120''$. The $H\alpha$ image shows the morphology of the flare.

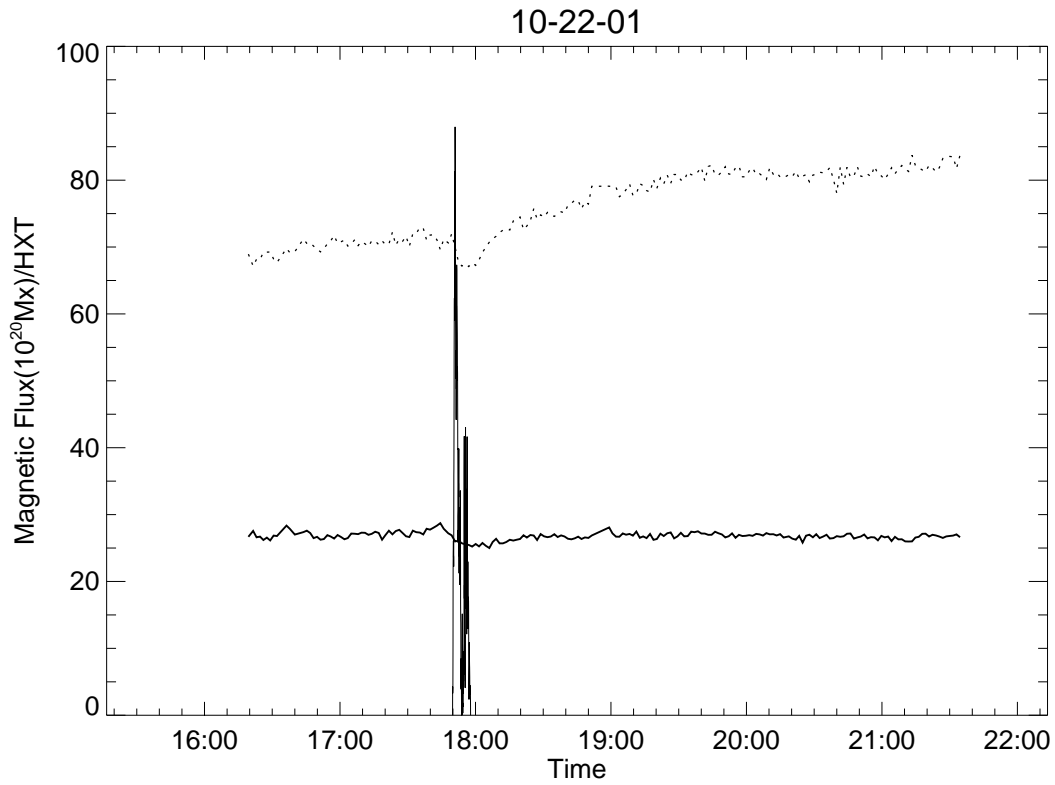


Fig. 10.— The evolution of line-of-sight magnetic flux in AR 9672 on October 22, 2001. The solid line represents the following (positive) flux while the dashed line represents the leading flux (negative). The thin solid line is the YOHKOH hard X-ray curve in high energy channel of HXT.